Investigation of Transition Metal Oxide Electron Transporting Layer for Inverted PM6:Y6 Polymer Solar Cells

Capstone Report

Zinedenova Aruzhan

Nazarbayev University
Department of Electrical and Computer Engineering
School of Engineering and Digital Sciences

This project report was created on TexStudio editing platform using LaTeX. All the figures were drawn using draw.io online software tool.

NAZARBAYEV UNIVERSITY

Electrical and Computer Engineering
Nazarbayev University
http://www.nu.edu.kz

Title:
Investigation of Transition Metal Oxide Electron Transporting Layer for Inverted PM6:Y6 Polymer Solar Cells

Theme:

Project Period:
Spring 2024

Project Group:

Participant(s):
Aruzhan Zinedenova

Supervisor(s):
Annie Ng

Copies: 1

Page Numbers: 19

Date of Completion:
April 26, 2024

Abstract:

The field of renewable energy has notably boosted over time, whereas the demand for more efficient and sustainable solar cell technologies is taking central attention. Among the various photovoltaic structures, organic photovoltaic (OPV) devices have emerged as promising candidates due to their cost-effectiveness, adaptability, and ease of management. However, the journey towards realizing the full potential of OPVs has been hindered by two critical challenges: rapid degradation and low efficiency. The issue of stability can be addressed by implementing another structural configuration, namely inverted OPV devices. In comparison to regular devices, inverted OPVs exhibit longer lifetimes, addressing the stability concern. Nevertheless, they suffer from low device efficiency. The primary goal of this research is to identify the proper materials among different metal oxides and to optimize them through multilayering, interlayering, and additive engineering for an efficient ETL structure for future flexible, integrated, and semitransparent electrode devices.

Contents

Preface

As the world have an urgent need for sustainable and efficient energy solutions, the field of renewable energy has gained unprecedented attention. Among the various avenues explored, the development of efficient solar cell technologies stands out as a promising path. This capstone project, undertaken at Nazarbayev University in the Department of Electrical and Computer Engineering, delves into the exploration of transition metal oxide electron transporting layers (ETLs) for inverted PM6:Y6 polymer solar cells.

This project presents a comprehensive study encompassing the selection, characterization, and optimization of metal oxides. The research methodology integrates a mix of experimental and analytical approaches, including additive and interface engineering, comparative efficiency assessments, and extensive data analysis. Our findings offer valuable insights into the development of more stable and efficient OPV devices, potentially contributing significantly to the field of renewable energy.

I extend my gratitude to my supervisor, Annie Ng, for her invaluable guidance and support throughout this project. I also thank my peers and the faculty at Nazarbayev University for their encouragement and constructive feedback.

As we move towards a future where sustainable energy is not just a necessity but a reality, it is my hope that this project adds a small but significant impact to the advancment of renewable energy technologies.

Nazarbayev University, April 26, 2024

Aruzhan Zinedenova
<Aruzhan.zinedenova@nu.edu.kz>

Chapter 1

Introduction

Polymer solar cell devices, also known as organic photovoltaic (OPV) devices, are utilized for converting sunlight into electricity. The distinct advantage of polymer solar cells lies in their accessibility, flexibility and potential to reduce the cost compared to conventional silicon devices [1].

The working principle of OPV devices is based on the photoelectric effect, which can be easily investigated. Upon exposure to sunlight, active photons stimulate the electrons within the bulk of the sandwiched device, causing them to move from their respective orbits, thereby creating an electron flow that generates electricity [2]. Consequently, the OPV became a full value energy converter device[2].

Polymer solar cells are mostly implemented for their flexibility, as they can be applied in a variety of devices, including photovoltaic cells and wearable devices[3]. However, these devices are faced with limitations regarding their power conversion efficiency and stability.

The focus of this Capstone project has been the careful selection and optimization of metal oxides to enhance organic photovoltaic technology. We began with an in-depth analysis of common metal oxides, namely zinc oxide, titanium dioxide, and tin dioxide, moving toward comparing the efficiency of single/multilayer metal oxide configurations, additive engineering with EMIM-DEP ionic liquid, and applying interlayers using PCBM, PMMA, and carbon-quantum dots (c-QD). These experimental approaches were used to examine the effects of multilayering on smoothing the surface of metal oxides after deposition, the impact of ionic liquid on the thermal stability of metal oxides, and interface engineering on optimizing energy level alignment between the ETL and the active layer, thus reducing carrier recombination. These investigative paths have been crucial in identifying the best configuration for organic photovoltaic cells, opening new possibilities for their wider application in renewable energy.

Chapter 2

Background

2.1 Architecture of Organic Photovoltaic Devices (OPV)

The effective performance of organic photovoltaics (OPV) is largely attributed to its sandwich-like structure, with an active layer situated between the electron transport layer (ETL) and hole transport layer (HTL). This structure can be configured in different ways, with the conventional structure consisting of a transparent conductive electrodes, namely fluorine tin oxide or indium tin oxide, a hole transporting layer, the active layer, an electron transport layer, and a metal electrode (Figure 2.1.) [4]. In contrast, the inverted structure includes an indium tin oxide layer, an ETL, the active layer, and a HTL (Figure 2.2) [5]

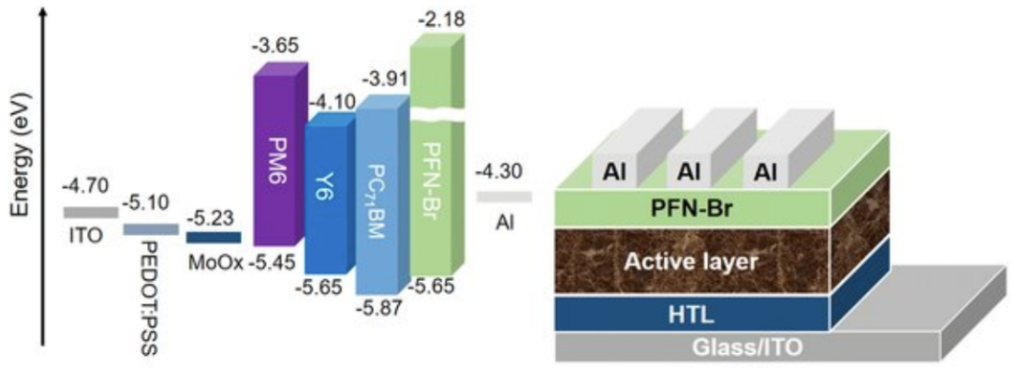

Figure 2.1: Prototype of Conventional Structure for OPV[5]

For this project, the inverted OPV structure is preferred due to its improved stability and resistance to moisture and oxygen, which reduces degradation and extends the cell's lifespan [6][7]. Additionally, the inverted OPV structure (Figure

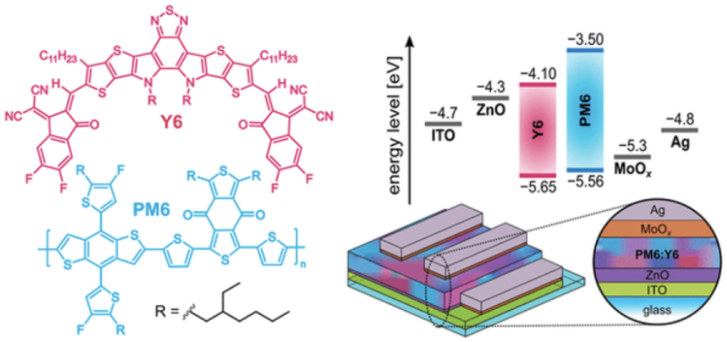

Figure 2.2: Prototype of Inverted Structure for OPV[5]

2.3) offers diverse applications, such as integration of perovskite solar cells (PSC) [8] and semi-transparent electrode device fabrication[2]. Although PSCs possess similar structural variations, their traditional structure is inverted relative to that of OPV, with inverted PSCs serving as the traditional polymer solar cell. The integration of traditional PSCs with OPV for the development of integrated solar cell devices is a promising avenue that offers benefits over commercially available silicon-based solar cells, including increased efficiency and reduced cost [8]. Regarding semi-transparent electrode devices, the inverted OPV structure have molybdenum trioxide as a HTL, which provides an opportunity to deposit transparent electrode for opaque devices. This OPV technologies have a promising future in vehicles and window applications[2].

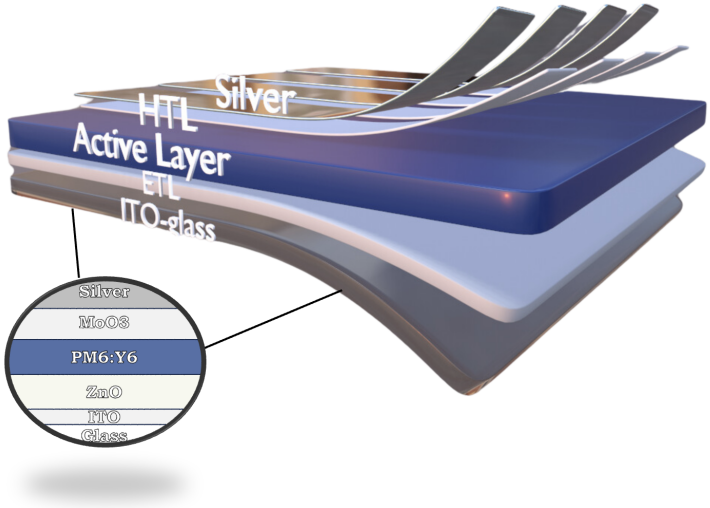

Figure 2.3: Structure of OPV and selected materials

It is important to note that organic photovoltaics (OPVs) have significant poten-

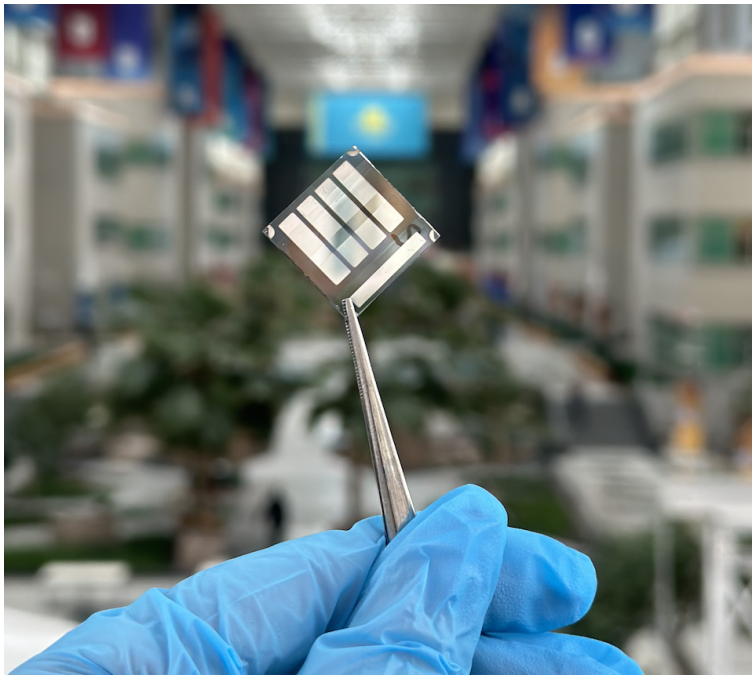

Figure 2.4: Fabricated OPV

tial for advancements in wearable and portable electronics [9]. For development in this direction, the mechanical properties of the fabricated cells must be considered. Therefore, OPVs are a fundamental solution because they are constructed with polymers in the ETL and HTL, which facilitates bending. According to Qin et al., conventional OPV structures demonstrate higher power conversion efficiency but suffer from lower stability, leading to rapid cell degradation [9]. In contrast, the inverted OPV structure offers a more promising alternative due to its enhanced stability. However, challenges arise with the use of metal oxides as ETLs, which are less flexible than polymers, leading to cracks that can extend to the active layer and HTL, creating dead areas as it is shown in Figure 2.5 [10]. Despite these issues, flexible conventional OPVs have achieved an efficiency of 11.35 % (Table 2.1) in laboratory conditions. To develop devices with higher resistance to moisture and oxygen, and significant efficiency, further optimization of the ETL in inverted OPVs is essential. This optimization could be a key development in the fabrication of flexible OPV with longer lifetime and promising efficiency.

Table 2.1: Flexible OPV parameters

Conditions	**Scan**	**Voc**, V	**Jsc**, $mA/cm2$	**FF**	**PCE**
PET/ITO/PEDOT:PSS/PM6:Y6/PNDIT-F3N-Br	for	0.78	20.87	69.30	11.35
	rev	0.78	20.94	69.46	11.40

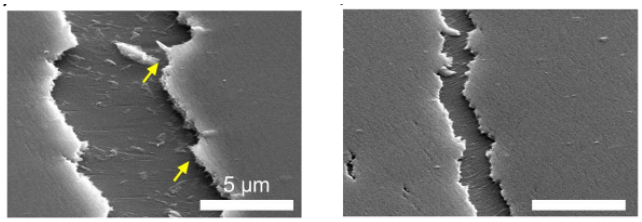

Figure 2.5: Cracks on flexible devices [10]

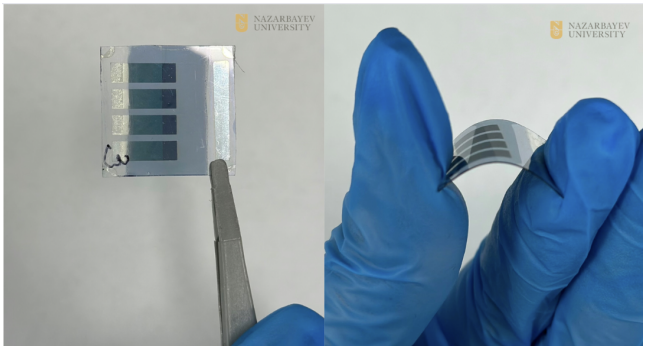

Figure 2.6: Flexible OPV

2.2 Stability of inverted OPV

In comparison to traditional OPV architectures, inverted OPV devices demonstrate superior lifetimes. The inverted OPV structure utilizes metal oxides like zinc oxide, titanium dioxide, and tin dioxide as ETL and molybdenum trioxide as HTL. These metal oxides possess higher work functions compared to the polymer materials typically used in conventional OPV structures[11]. Notably, both the ETL and HTL materials in inverted OPV devices are non-acidic, thereby minimizing the risk of degradation acceleration. Conversely, conventional OPV devices face a stability challenge with the use of PEDOT:PSS as the HTL. While PEDOT:PSS contributes to high performance, its hygroscopic property leads to moisture absorption from the surrounding environment, compromising stability. In order to protect the devices from different enviromental factors and increase its durability, the fabricated cells encapsulated with glass and epoxy glue[12]. The aging trends of both inverted and conventional OPV were systematically observed over 9 weeks by weekly measuring with solar simulator to assess their stability under ambient environmental conditions, as illustrated in Figure 2.7. The graph demonstrates that the efficiency of inverted and traditionally structured OPVs are reduced for almost 10 and 30 percent, respectively. The obtained results show that theoretical expectations about the stability of two configurations are true.

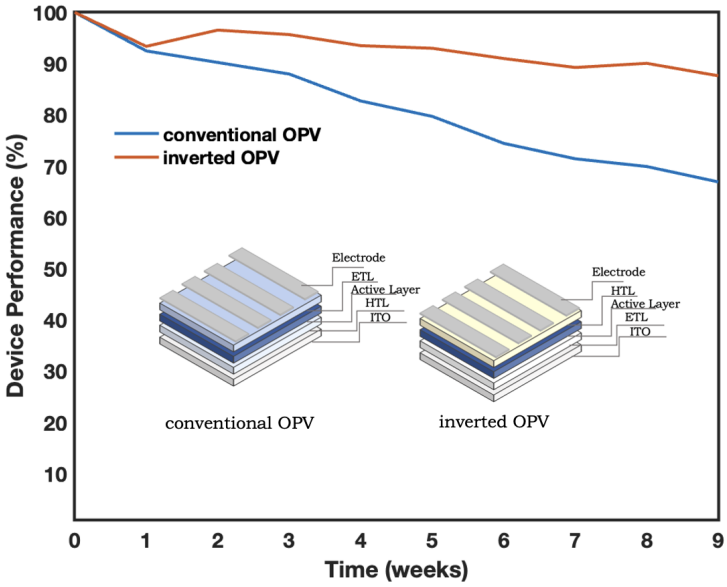

Figure 2.7: The device performance during 9 weeks of remeasuring

2.3 PM6:Y6 characterization

Recent research has indicated that the PM6:Y6 structure is the most efficient configuration as an active layer for OPV devices, employing a typical bulk heterojunction strategy. Both PM6 and Y6 are polymers within a strong infrared light absorption spectra [6]. A narrow optical band gap is present between the two polymers, as illustrated in Figure 2.8, where the highest occupied molecular orbital (HOMO) and lowest unoccupied molecular orbital (LUMO) energy levels are -5.65 eV for Y6 and -5.54 eV for PM6, as well as -4.10 eV for Y6 and -3.65 eV for PM6, respectively [2].

The PM6:Y6 polymer combination is considered "well-complementary" when the HOMO level of one polymer aligns closely with the LUMO level of the other, resulting in an efficient charge transfer complex formation at the interface [2] [13]. As polymers consist of long chain repeating groups of atoms, the electrons along chain approach the other polymer upon contact, creating a "meeting point" where electron transfer occurs[14]. The formation of such a charge transfer contributes significantly to high conductivity and separation of positive and negative charges, which is activating photovoltaic effect described in device performance [15]. Due to their well-complementary combination, PM6 and Y6 are frequently utilized as the active layer in OPV devices[16].

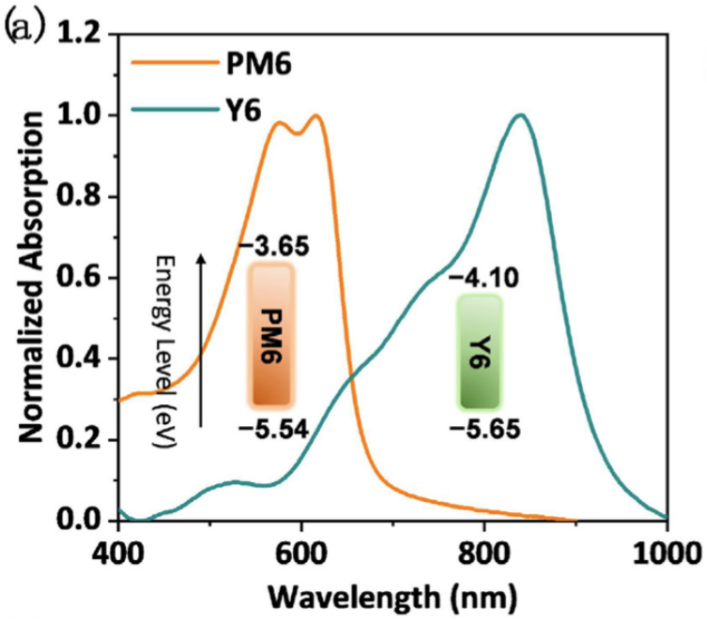

Figure 2.8: Energy band diagram of PM6 and Y6[4]

2.4 Different Electron Transport Layer characterization

The incorporation of well-complementary polymers is essential for efficient photon-to-electron conversion in both inverted and conventional organic photovoltaic (OPV) devices [1]. However, in order to achieve optimal performance in polymer solar cells, it is necessary to address the trade-off between electron and hole transport layers. The primary objective of this project is to investigate the potential of metal oxide layers for the fabrication of integrated devices.

Existing studies [17][18] indicate that metal oxides, such as zinc oxide and titanium dioxide, are commonly employed as electron transport layers (ETLs) in polymer and perovskite solar cells. Various preparation and deposition techniques are available for these metal oxides [17]. In this study, we will utilize commercialized zinc oxide nanoparticles, which offers unique advantages over traditional zinc oxide due to its small particle size. The nanoparticles in this ink are less than 100 nanometers in diameter and are present in a liquid or viscous state[19]. The high surface area-to-volume ratio of nanoparticles contributes to enhanced physical and mechanical properties, as well as increased reactivity [19]. Another reason for utilizing commercialized zinc oxide is the potential to establish a reproducible fabrication process for stable devices, while the titanium dioxide will be synthesized by hand in a lab. As the aim of this project suggests, the paper will represent

the affordable and reproducible preparation process of OPV devices.

Also, according to the energy band diagram presented by Zhu and Hu [20] in Figure 2.9, the titanium dioxide and zinc oxide are in the same level, therefore they will-complement the polymer blend solution's HOMO and LUMO characteristics (Figure 2.8). However, the compatibility of tin dioxide with PM6 under the suspission of succesful ETL application, because of misalignment in energy band diagram. Moreover, it's crucial to address the compatibility challenges between zinc oxide and polymers when they are employed as ETLs in organic electronic devices. While zinc oxide effectively matches the LUMO of acceptor materials, its hydrophilic nature contrasts with the hydrophobic nature of most polymers, causing the low contact angle during the active layer deposition[21]. Therefore, optimizing the ETL is pivotal for enhancing device efficiency. This capstone project is dedicated to exploring and optimizing ETLs through multilayering, interlayering and additive engineering techniques to address compatibility concerns and enhance device performance.

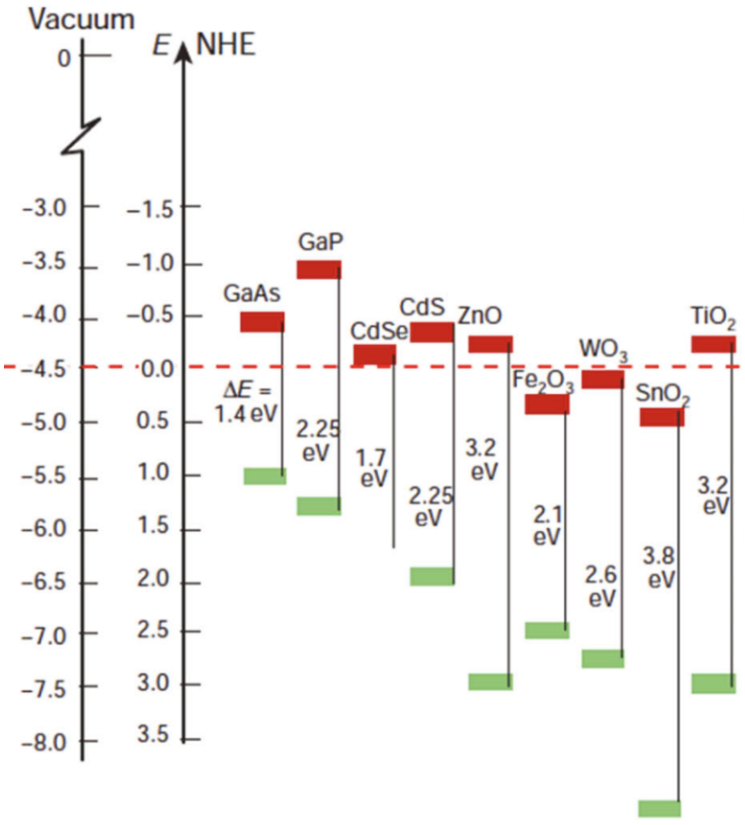

Figure 2.9: Different Metal Oxide's energy band diagram[20]

Chapter 3

Methodology

3.1 Methods and Procedure of Data Collection

I. Literature Review:

Conduct an extensive literature review to gain a comprehensive understanding of the current state of organic photovoltaic (OPV) technology, including its challenges, recent advancements, and the role of ETL optimization. The fabrication method for the whole device structure established after careful examination of device fabrication techniques proposed by several sources. Moreover, to save time, the selection of metal oxides, polymers, and ionic liquids for the experiments conducted in this project will be based on their properties and compatibility as described in the literature for the future architecture of OPV devices.

II. Material Selection:

Select ETL materials based on their compatibility with the chosen polymer materials and their ability to enhance charge transport. Compare commercially available zinc oxide nanoparticles ink., tin dioxide and synthesized titanium dioxide.

III. Preparation:

The research project starts from investigating the proper fabrication process of a polymer solar cell. The process involved cleaning, synthesis, device fabrication, J-V curve measurement and characterization.

a. Cleaning

Fluorine-doped tin oxide (FTO) and indium-doped tin oxide (ITO) substrates cleaning conducted using detergent, deionized water, acetone, and isopropyl alcohol through sonication for 20 minutes each. Following the cleaning, the substrates were dried blowing the nitrogen and treated under ultra-violet (UV) ozone for 30 minutes [18].

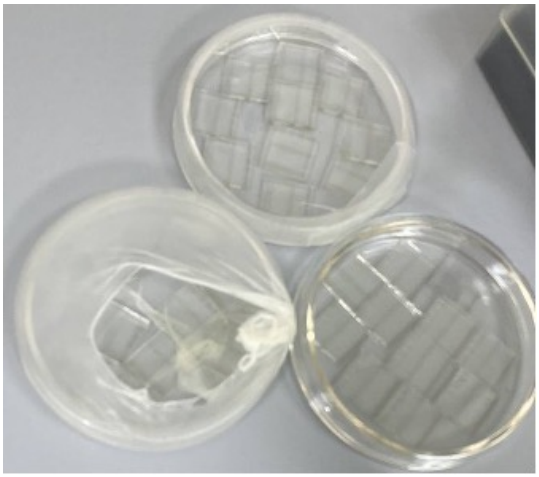

Figure 3.1: Clean Substrates

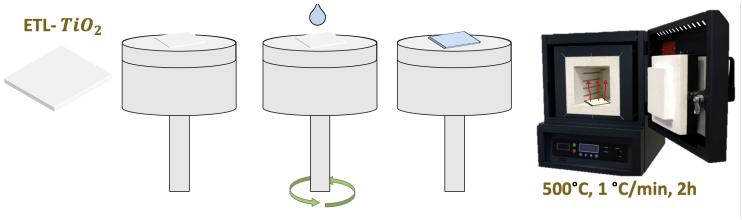

Figure 3.2: Titanium dioxide deposition

b. Synthesis of titanium oxide

The mixed solution of Polyvinylpyrrolidone (PVP) in Isopropyl alcohol (IPA) and acetic acid was added drop-by-drop into the Titanium isopropoxide (TTIP) in IPA solution with acetic acid during the magnetic stirring. The prepared titanium oxide treated at high thermal annealing temperature in the oven at 500 degree as it is shown in Figure 3.2.

c. Device Fabrication

The active layer solution with PM6:Y6 prepared at a weight ratio of 1:1.2 and stirred for 3 hours at room temperature using a magnetic stirrer[2]. Chloronaphthalene was added to the active layer solution 30 minutes before the deposition process. The zinc oxide nanoparticles were tested together with zinc oxide compact layer which id synthesized by hand. However, as previously mentioned, to ensure reproducibility in this project, commercially available nanoparticles were used to prepare the electron transport layer. This decision was made because the hand-synthesized solutions showed different results in each experiment. As it is shown in Figure 3.3, the zinc oxide ink. was sonicated for 30 minutes and de-

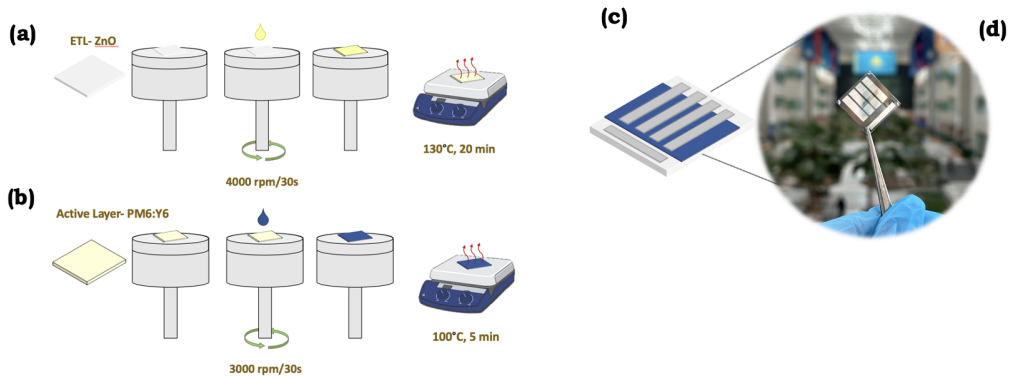

Figure 3.3: (a) Deposition of Electron Transport Layer (Zinc oxide); (b) Deposition of Active Layer (PM6:Y6); c) Thermal Evaporation of Molybdenum trioxide and Silver; (d) Fabricated OPV device.

posited in a fume hood in air at 4000 rpm for 30 seconds, followed by annealing at 130 degrees for 20 minutes. Subsequently, the PM6:Y6 solution was deposited at 3000 rpm for 30 second on top of titanium dioxide and zinc oxides, and annealed at 100 degrees for 5 minutes. Finally, molybdenum trioxide and silver were thermally deposited onto the prepared substrates with thicknesses of 100 Å and 1000 Å, respectively[22].

3.2 Methods and Procedure of Data Analysis

Characterization Techniques:

a. The J-V curve measurement will be conducted on the fabricated device using a Solar Simulator in an ambient environment. This procedure aims to obtain the J-V curve of each device, allowing for comprehensive characterization.

b. EQE and IQE. The external quantum efficiency measuring will be used to define the amount of photons converted to the electron at specific wavelength. This characterization also will be applied to show that the carriers mobility increased and caused increase in current density.

c. PAS attain the predetermined objective of achieving high stability in inverted OPV devices. To assess the efficiency of these devices under UV light, the PAS equipment monitor and control the lifetime of prepared inverted OPVs.

Chapter 4

Results and Discussions

4.1 Results

Table 4.1: Summary of inverted OPVs with ETL multilayering

Conditions	Scan	Voc, V	Jsc, $mA/cm2$	FF	PCE
FTO/ZnO/PM6:Y6/MoO3	for	0.79	20.25	60.45	8.89
	rev	0.75	20.10	57.17	8.55
FTO/TiO2/PM6:Y6/MoO3	for	0.77	16.93	63.44	8.64
	rev	0.76	16.64	63.62	8.50
FTO/ZnO/ZnO/PM6:Y6/MoO3	for	0.83	21.37	59.49	10.06
	rev	0.83	21.35	59.71	10.66
FTO/TiO2/TiO/PM6:Y6/MoO3	for	0.78	14.73	54.83	6.37
	rev	0.78	14.68	55.17	6.39
FTO/ZnO/ZnO/ZnO/PM6:Y6/MoO3	for	0.83	21.54	55.85	9.99
	rev	0.83	21.55	56.25	10.06
FTO/TiO2/ZnO/PM6:Y6/MoO3	for	0.82	21.62	65.83	**11.707**
	rev	0.82	21.59	65.95	11.705

Table 4.2: Summary of additive engineering

Conditions	Scan	Voc, V	Jsc, $mA/cm2$	FF	PCE
FTO/ZnO/PM6:Y6/MoO3	for	0.77	24.59	52.43	10.06
	rev	0.76	16.64	63.62	9.91
FTO/TiO2/PM6:Y6/MoO3	for	0.77	17.10	60.68	8.093
	rev	0.77	17.07	60.71	8.074
FTO/ZnO+EMIM-DEP/PM6:Y6/MoO3	for	0.73	23.98	48.88	8.71
	rev	0.74	24.24	50.30	9.13
FTO/TiO2+EMIM-DEP/PM6:Y6/MoO3	for	0.76	16.31	52.42	6.58
	rev	0.75	16.51	47.97	5.99

Table 4.3: Summary of interlayering

Conditions	Scan	Voc, V	Jsc, $mA/cm2$	FF	PCE
ITO/ZnO/PM6:Y6/MoO3	for	0.81	22.63	71.15	12.99
	rev	0.81	22.64	71.09	13.00
ITO/ZnO/PCBM/PM6:Y6/MoO3	for	0.81	18.55	73.87	11.00
	rev	0.81	18.44	73.00	10.95
ITO/ZnO/PCBM:PMMA/PM6:Y6/MoO3	for	0.82	22.38	68.79	12.62
	rev	0.82	22.26	69.01	12.59
ITO/ZnO/c-QD/PM6:Y6/MoO3	for	0.82	23.30	73.80	**14.03**
	rev	0.82	23.27	73.87	**14.02**

4.2 Discussions

The investigation into efficient ETL materials began with a material selection process. Initially, common metal oxides such as zinc oxide, tin dioxide, and titanium dioxide were examined for their suitability. These materials were deposited on FTO substrates to evaluate their performance. Zinc oxide and titanium dioxide show compatibility of layers according to the results in Table 4.1 and Table 4.2, while tin oxide's performance lagged due to the energy level gap between ETL and PM6, as it was predicted in background section based on Figure 2.9.

In the next stage, the commercial zinc oxide nanoparticles compared with zinc oxide compact layer prepared by hand. However, the experiment show better power conversion efficiency with higher current density and reproducible efficiency results using the zinc oxide from Sigma Aldrich. Based on that results, the zinc oxide purchased from Sigma Aldric recommended for further experiments, considering its stability and efficiency.

The optimization of ETL for inverted OPV devices, as detailed in **Table 4.1**, the focused on multilayering of selected metal oxides, hypothesizing that this approach could enhance device performance. The adoption of double, triple ETL coatings aimed to reduce the surface roughness and improving the charge transfer[23]. This strategy was expected to significantly improve the device's efficiency by minimizing the recombination of charge carriers within the bulk, effectively enhancing hole-blocking capabilities. However, the study also uncovered a challenge with titanium dioxide: its efficiency was notably compromised under high thermal annealing conditions at 500 degrees, where deposition of second layer contributes to the second thermal annealing of the substrate impacting on degradation of ETL's first layer. To address this, a novel method of layering zinc oxide atop titanium dioxide was introduced, yielding the most favorable results with an efficiency enhancement up to 11.7%. This combination of zinc and titanium dioxide, optimized

the current density for the control device accounting for 20.25 mA/cm2 to 21.62 mA/cm2.

Table 4.2 shows the results of incorporating ionic liquids into the ETLs. The 1-Ethyl-3-methylimidazoliumdiethyl phosphate (EMIM-DEP) ionic liquid was tested in various concentrations to mitigate material degradation during high-temperature annealing [24]. Despite the theoretical advantages, this method did not produce significant improvements. Therefore, the focus of next experiments move to study interface engineering techniques to enhance device performance and reduce contamination risks.

According to **Table 4.3**, the next method of ETL optimization involved the interlayering of PCBM, PCBM:PMMA mixture, and carbon-quantum dots (c-QD) between zinc oxide and the active layer. For this approach the FTO substrates substituted with ITO substrates. This change was motivated by findings indicating that ITO surfaces are smoother with lower sheet resistance, offering the potential for higher power conversion efficiency. Given that FTO substrates were initially chosen for their resistance to high annealing temperatures required for the titanium dioxide layer, there was no necessity to retain FTO substrates for the selected metal oxide, namely zinc oxide. Therefore, the interlayering technique was implemented using ITO substrates.

From the obtained results, it is evident that PCBM and PCBM:PMMA did not demonstrate a significant increase in efficiency, resulting significant reduction of either current density or fill factor, while the c-QD showed promising improvements. As depicted in the J-V curve in Figure 4.1, the c-QD exhibited an increase in open-circuit voltage (Voc) of 0.82, a short-circuit current density (Jsc) of 23.30 mA/cm2, a fill factor (FF) of 73.80, and a power conversion efficiency (PCE) of 14.03%. In comparison, the reference device had a Voc of 0.81, a Jsc of 22.63 mA/cm2, an FF of 71.15, and a PCE of 12.99%.

The EQE spectra were measured for both the inverted reference and the bilayer ZnO/c-QD OPV. According to the referenced article, the presence of c-QD contributes to the smoother deposition of the active layer, thereby improving the contact quality between the ETL and the active layer [25]. The study indicates that better contact quality reduces recombination in the bulk, leading to a maximum EQE of 87% at wavelengths around 650 nm[25]. This trend is also evident in Figure 4.2, where the inverted OPV with c-QD exhibits a maximum EQE of approximately 73% at a wavelength of 630 nm. A higher EQE at a specific wavelength indicates that more photons are being converted into electrons, which correlates with a higher current density[25]. Therefore, EQE of the interlayered device has

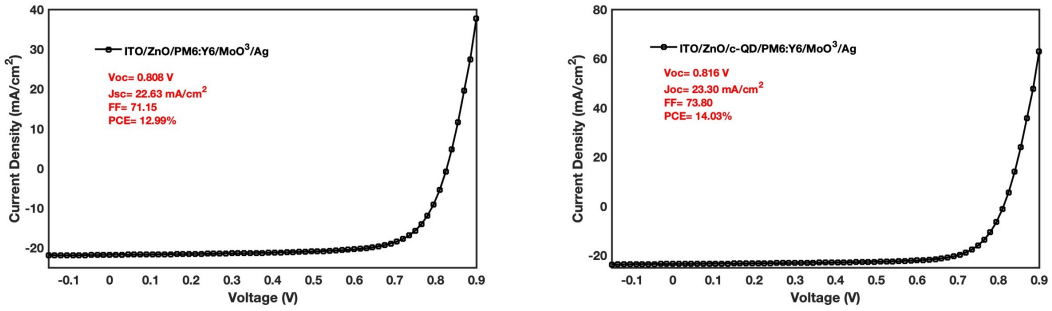

Figure 4.1: J-V curve data for OPV (a) reference cell; (b) carbon-quantum dots as an interlayer.

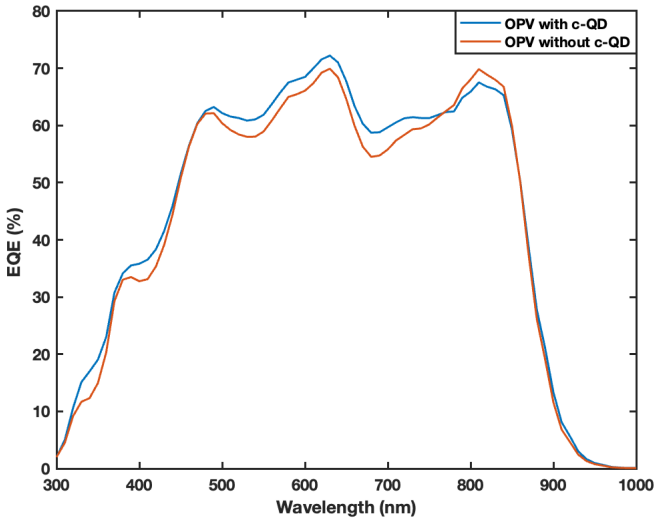

Figure 4.2: EQE characteristics

been compared with the reference device at certain wavelengths, suggesting that the c-QD device is generating a higher current density at a wavelength accounting 630 nm.

Chapter 5

Conclusion

The development of the efficiency and stability of inverted PM6:Y6 polymer solar cells through the optimization of metal oxides in ETL has been discussed extensively. The study has pointed out that using zinc oxides as an ETL offers better efficiency and reproducibility than applying other metal oxides, namely self-synthesized titanium dioxide and commercially available tin dioxide.

Comparing to multilayer configurations of zinc oxide and titanium dioxide, additive engineering with EMIM-DEP, carbon quantum dot (c-QD) interlayer optimization technique has led to the achievement of maximum efficiency of 11% and 14% for inverted OPV, respectively. This is primarily seen in enhanced charge transfer efficiency and improved resistance to environmental degradation. The innovative approach of c-QD on zinc oxide emerged as a key finding, demonstrating a remarkable boost in device efficiency. Although multilayering and additive engineering techniques did not substantially improved the device performance, they offered notable insights for future exploration.

The project's outcomes not only contribute to the advancement of OPV technology but also underscore the potential of these findings in broader applications like flexible device fabrication, semi-transparent electrode deposition [26] and next-generation photovoltaics with perovskite/organic integration [27]. These contributions are poised to influence a wide range of future developments in photovoltaic technology.

Bibliography

[1] Instrumentation Energy IEEE International Conference on Power and Control (PIECON), eds. *Parameter Extraction Of Organic Solar Cell: A Review*. 2023. DOI: 10.1109/PIECON56912.2023.10085878.

[2] R. Yu, G. Wu, and Z. Tan. "Realization of high performance for PM6:Y6 based organic photovoltaic cells". In: *Journal of Energy Chemistry* 61 (2021). DOI: 10.1016/j.jechem.2021.01.027.

[3] C. Sealy. "Materials Today". In: *Promising Power Source for Wearable Electronics* (2023). DOI: 10.1016/j.mattod.2014.10.006.

[4] Y. Gong et al. "Water-Induced Formation of MoO3 Microcrystals as Anode Buffer Layer for Highly Efficient Polymer Solar Cells". In: *Energy Technology* 9.12 (2021). DOI: 10.1002/ente.202100718.

[5] B. R. Luginbuhl et al. "Resolving atomic-scale interactions in nonfullerene acceptor organic solar cells with solid-state NMR spectroscopy, crystallographic modelling, and molecular dynamics simulations". In: *Advanced Materials* 34.6 (2022). DOI: 10.1002/adma.202105943.

[6] M. Fernandez-Castro, M. Espindola-Rodriguez J. Truer, and J. W. Andreasen. "Environmentally Friendly and Roll-Processed Flexible Organic Solar Cells Based on PM6: Y6". In: *Frontier in Nanotechnology* 4 (2022), pp. 1–11. DOI: 10.3389/fnano.2022.885138.

[7] M. Cui et al. "A Cost-Effective, Aqueous-Solution-Processed Cathode Interlayer Based on Organosilica Nanodots for Highly Efficient and Stable Organic Solar Cells". In: *Advanced Materials* 32.38 (2020). DOI: 10.1002/adma.202002973.

[8] X. He et al. "Enhancing Photoresponse and Photocurrent of Integrated Perovskite/Organic Solar Cells via Layer-by-Layer Processing". In: *ACS Applied Energy Materials* 6.2 (2023), pp. 981–988. DOI: 10.1021/acsaem.2c03425.

[9] Qin Jianqiang et al. "Recent progress in flexible and stretchable organic solar cells". In: *Advanced Functional Materials* 30.36 (2020). DOI: 10.1002/adfm.202002529.

[10] Lee Seungbok et al. “Intrinsically Stretchable Organic Solar Cells without Cracks under 40% Strain”. In: *Advanced Energy Materials* 13.30 (2023). DOI: 10.1002/aenm.202300533.

[11] William R. Mateker and Michael D. McGehee. “Progress in Understanding Degradation Mechanisms and Improving Stability in Organic Photovoltaics”. In: *Advanced Materials* 29.10 (). DOI: 10.1002/adma.201603940.

[12] Ebru Kondolot Solak and Erdal Irmak. “Advances in organic photovoltaic cells: a comprehensive review of materials, technologies, and performance”. In: *Royal Society of Chemistry* 13.18 (2023). DOI: 10.1039/D3RA01454A.

[13] Guo Qing et al. “Recent advances in PM6: Y6-based organic solar cells”. In: *Materials Chemistry Frontiers* 5.8 (2021). DOI: 10.1039/D1QM00060H.

[14] J. Hou et al. “Organic solar cells based on non-fullerene acceptors”. In: *Nat. Mater* 17 (2018), pp. 119–128. DOI: 10.1038/nmat5063.

[15] Bing-Huang Jiang et al. “High-Performance Semitransparent Organic Photovoltaics Featuring a Surface Phase-Matched Transmission-Enhancing Ag/ITO Electrode”. In: *ACS Appl. Mater. Interfaces* 12 (2020). DOI: doi.org/10.1021/acsami.0c10906.

[16] Y. Zhang, Y. Lang, and G. L. “Recent advances of non-fullerene organic solar cells: From materials and morphology to devices and applications”. In: *EcoMat* 5.1 (2022). DOI: 10.1002/eom2.12281.

[17] Sandro Lattante. “Electron and Hole Transport Layers: Their Use in Inverted Bulk Heterojunction Polymer Solar Cells”. In: *Electronics* 3.1 (2014), pp. 132–164. DOI: 10.3390/electronics3010132.

[18] Stefan Schumann et al. “Inverted organic photovoltaic devices with high efficiency and stability based on metal oxide charge extraction layers”. In: *Journal of Materials Chemistry* 21.7 (2011), pp. 2381–2386. DOI: 10.1039/C0JM03048A.

[19] Chunhui Liu, Chengyi Xiao, and Weiwei Li. “Zinc oxide nanoparticles as electron transporting interlayer in organic solar cells”. In: *Journal of Materials Chemistry C* 9.40 (2021). DOI: 10.1039/D1TC03434K.

[20] Feng Zhu et al. “Amorphous silicon carbide photoelectrode for hydrogen production from water using sunlight”. In: *Solar Energy* 89 (2010). DOI: 10.1080/14786430902740729.

[21] Song Yang and Huangzhong Yu. “The modification of ZnO surface with natural antioxidants to fabricate highly efficient and stable inverted organic solar cells”. In: *Chemical Engineering Journal* 452.4 (2023). DOI: 10.1016/j.cej.2022.139658.

[22] Sebastian Pont et al. “Stability of Polymer:PCBM Thin Films under Competitive Illumination and Thermal Stress”. In: *Advanced Functional Materials* 28 (2018). DOI: 10.1002/adfm.201802520.

[23] J. Song et al. “Ternary organic solar cells with efficiency > 16.5% based on two compatible nonfullerene acceptors”. In: *Advanced Materials* 31.52 (2019). DOI: 10.1002/adma.201905645.

[24] Zheng Xiaojia, Wei Yu, and Shashank Priya. “Interfacial charge-transfer engineering by ionic liquid for high performance planar CH3NH3PbBr3 solar cells”. In: *Journal of energy chemistry* 27.3 (2018). DOI: 10.1016/j.jechem.2017.09.016.

[25] Ruqin Zhang et al. “Solution-Processable ZnO and Carbon Quantum Dots Electron Extraction Layer for Highly Efficient Polymer Solar Cells”. In: *ACS Applied Materials and Interfaces* 10.5 (2018). DOI: 10.1021/acsami.7b17969.

[26] Wachsmuth Josua et al. “Fully Printed and Industrially Scalable Semitransparent Organic Photovoltaic Modules: Navigating through Material and Processing Constraints”. In: *Solar RRL* 7.20 (2023). DOI: 10.1002/solr.202300602.

[27] Sun Shuang-Qiao et al. “All-Inorganic Perovskite-Based Monolithic Perovskite/Organic Tandem Solar Cells with 23.21% Efficiency by Dual-Interface Engineering”. In: *Advanced Energy Materials* 13 (16 2023). DOI: 10.1002/aenm.202204347.